Cell Metabolism
Article

Arcuate NPY Controls Sympathetic Output and BAT Function via a Relay of Tyrosine Hydroxylase Neurons in the PVN

Yan-Chuan Shi,[1,6] Jackie Lau,[1] Zhou Lin,[1] Hui Zhang,[1] Lei Zhai,[1] Guenther Sperk,[2] Regine Heilbronn,[3] Mario Mietzsch,[3] Stefan Weger,[3] Xu-Feng Huang,[4] Ronaldo F. Enriquez,[1] Lesley Castillo,[1] Paul A. Baldock,[1] Lei Zhang,[1] Amanda Sainsbury,[1,5,7,8] Herbert Herzog,[1,6,8,*] and Shu Lin[1,6,8]

[1]Neuroscience Division, Garvan Institute of Medical Research, 384 Victoria Street, Darlinghurst, Sydney, NSW 2010, Australia
[2]Department of Pharmacology, Medical University Innsbruck, 6020 Innsbruck, Austria
[3]Institute of Virology, Campus Benjamin Franklin, Charité Universitätsmedizin Berlin, 12203 Berlin, Germany
[4]School of Health Science, Illawarra Health and Medical Research Institute, University of Wollongong, NSW 2522, Australia
[5]School of Medical Sciences
[6]Faculty of Medicine
University of New South Wales, Sydney, NSW 2052, Australia
[7]The Boden Institute of Obesity, Nutrition, Exercise, and Eating Disorders, The University of Sydney, NSW 2006, Australia
[8]These authors contributed equally to this work
*Correspondence: h.herzog@garvan.org.au
http://dx.doi.org/10.1016/j.cmet.2013.01.006

SUMMARY

Neuropepetide Y (NPY) is best known for its powerful stimulation of food intake and its effects on reducing energy expenditure. However, the pathways involved and the regulatory mechanisms behind this are not well understood. Here we demonstrate that NPY derived from the arcuate nucleus (Arc) is critical for the control of sympathetic outflow and brown adipose tissue (BAT) function. Mechanistically, a key change induced by Arc NPY signaling is a marked Y1 receptor-mediated reduction in tyrosine hydroxylase (TH) expression in the hypothalamic paraventricular nucleus (PVN), which is also associated with a reduction in TH expression in the locus coeruleus (LC) and other regions in the brainstem. Consistent with this, Arc NPY signaling decreased sympathetically innervated BAT thermogenesis, involving the downregulation of uncoupling protein 1 (UCP1) expression in BAT. Taken together, these data reveal a powerful Arc-NPY-regulated neuronal circuit that controls BAT thermogenesis and sympathetic output via TH neurons.

INTRODUCTION

Obesity occurs when there is a significant imbalance between energy intake and energy expenditure (Rosen and Spiegelman, 2006). While energy intake is almost entirely determined by food intake, energy expenditure is composed of several components, including basal metabolism, physical activity, and thermogenesis (Rosen and Spiegelman, 2006). Reduced adaptive thermogenesis has been reported to be responsible for reduced energy expenditure during energy deficit, as in weight loss programs (Major et al., 2007). In recent years, more focused research into the regulation of thermogenesis, particularly brown adipose tissue (BAT) thermogenesis, has indicated that BAT is under tight control by the central nervous system (CNS) (Whittle et al., 2011), of which the hypothalamus, and in particular the arcuate nucleus (Arc), has attracted special attention.

The Arc contains two major populations of neurons that are known to regulate energy balance: orexigenic neuropeptide Y (NPY)/agouti-related peptide (AGRP)-containing neurons, and anorexigenic proopiomelanocortin (POMC)/cocaine and amphetamine-regulated transcript (CART)-containing neurons (Lin et al., 2004) (Hahn et al., 1998). Activation of NPY/AGRP neurons leads to the release of NPY and AGRP, which strongly stimulate appetite and, when chronically elevated, lead to the development of obesity (Ellacott and Cone, 2004). This occurs via signaling of NPY on Y receptors, notably Y1 and Y5 receptors (Nguyen et al., 2012), as well as via the ability of AGRP to antagonize melanocortin 3/4 (MC3/4) receptors (Ellacott and Cone, 2004). Consistent with an important role of NPY in the regulation of energy homeostasis, chronic intracerebroventricular (i.c.v.) or hypothalamus-specific administration of NPY to rodents leads to hyperphagia, accompanied by accelerated body weight gain, hyperleptinemia, hypercorticosteronemia, hyperinsulinemia, and increased adiposity (Sainsbury et al., 1997a; Zarjevski et al., 1993). More importantly, all of these neuroendocrine and metabolic effects of central NPY administration, notably increased adiposity, persist even when NPY-induced hyperphagia is prevented by pair feeding (Sainsbury et al., 1997b; Zarjevski et al., 1993). This indicates that hyperphagia is not the only mechanism by which central NPY increases adiposity and demonstrates that hypothalamic NPY must also alter other processes, such as energy expenditure, that contribute to the increased adiposity. In addition, elevated NPY-ergic tone and decreased adaptive thermogenesis during energy restriction and weight loss intervention suggest a possible relationship between Arc NPY signaling and adaptive thermogenesis (Major et al., 2007).

Despite the number of studies documenting the effects of central NPY administration on energy homeostasis, the

molecular mechanisms underlying these effects, including central and peripheral signaling pathways, are yet to be elucidated. One mechanism by which Arc NPY may decrease energy expenditure is through interaction with the sympathetic nervous system (SNS). Interestingly, increased hypothalamic NPY expression has been shown in animal models of obesity (Lin et al., 2000), and elevated circulating NPY levels have been found in obese women (Baranowska et al., 2005; Milewicz et al., 2000). On the other hand, many obesity syndromes are also associated with low sympathetic activity (Bray and York, 1998). While the relationship between Arc NPY and the SNS has been postulated, with demonstrations that hypothalamic NPY administration reduces sympathetic firing rate (Lundberg et al., 1989) or reduces sympathetically mediated processes such as BAT thermogenesis (Egawa et al., 1991), there is little known about the pathways involved or the underlying mechanism that controls it.

BAT has gained interest as a possible target for the normal control and treatment of obesity in adult humans via modulation of cold-induced and adaptive thermogenesis (Stephens et al., 2011). Moreover, there is an inverse correlation between the amount of BAT and body mass index in humans, with obese individuals having significantly less BAT than lean individuals (Virtanen et al., 2009). Considering the critical role that Arc NPY plays in the control of energy homeostasis, together with the fact that pair-fed animals with elevated Arc NPY levels still develop obesity (Sainsbury et al., 1997b; Zarjevski et al., 1993), we aimed to determine the brain circuits via which Arc NPY controls energy expenditure and SNS activity and subsequently modulates BAT activity. To this end, we utilized mouse models in which NPY is only produced in the Arc ectopically as well as more specifically only in Arc NPY neurons while it is absent everywhere else. This was achieved by adeno-associated virus (AAV)-mediated neuronal expression of NPY specifically in the Arc of NPY knockout ($NPY^{-/-}$) mice as well as AAV-FLEX-NPY-mediated Arc-NPY-specific expression in NPYCre knockin mice. $NPY^{-/-}$ mice were used because they enabled us to specifically dissect the role of Arc NPY independently of effects of other central or peripheral NPY pathways. Knowledge of the central regulation of BAT functionality gained from these experiments using techniques that are impossible in humans provides new information relevant to the control of energy homeostasis in humans.

RESULTS

Long-Term High-Fat Feeding Induces Elevation of Arc NPY mRNA Expression

Under normal conditions, Arc NPY expression is controlled by peripheral factors such as leptin and insulin and satiety factors like peptide YY (PYY), all of which reduce Arc NPY messenger RNA (mRNA) levels thus signaling a positive energy balance (Batterham et al., 2002; Elmquist et al., 1998; Marks et al., 1990). On the other hand, fasting and ghrelin action promote the opposite: an upregulation of Arc NPY mRNA levels, which signal negative energy balance and trigger an increase in appetite and a reduction in energy expenditure (Kamegai et al., 2000; Sainsbury and Zhang, 2010). This was evident in the Arc of wild-type (WT) mice after a 24 hr fasting period, which showed significantly elevated NPY mRNA expression (Figure 1Aa), compared to that in nonfasted chow-fed mice (Figure 1Ac). Paradoxically, these principles no longer apply under conditions of long-term overfeeding as seen in mice fed a high-fat diet for 20 weeks, in which Arc NPY mRNA expression was also significantly increased compared to chow-fed controls (Figures 1Ab and 1Ac). These results suggest that the dysregulated Arc NPY levels present in the high-fat-fed animals mimic an energy-deficit state that most likely exacerbates the already established obesity due to a further increase in food intake and reduction in energy expenditure, highlighting the critical importance of the Arc NPY system under obese conditions.

Mouse Models for Specific Expression of NPY Only in the Arc

In order to recapitulate the changes in energy expenditure under conditions of energy-deficit or long-term high caloric intake, and to specifically characterize the neuronal pathways involved in Arc NPY-induced reduction in energy expenditure and thermogenesis, we generated mouse models in which NPY is either overproduced in WT mice specifically in the Arc or selectively reintroduced into the Arc of otherwise NPY-deficient mice. We injected a recombinant adeno-associated virus that expresses NPY under a neuron-specific promoter (AAV-NPY) into the Arc of 11-week-old WT or germline $NPY^{-/-}$ mice (hereafter referred to as *WT+NPY* or *ArcNPY*, respectively) using an empty AAV (AAV-empty) as a control (hereafter referred to as *WT+empty* or $NPY^{-/-}$*+empty*, respectively). Viral delivery was targeted to just next to the Arc to avoid destruction of the nucleus, but close enough to allow diffusion of the virus into the Arc (right side of Figure 1Ba and higher-magnification of the boxed area in Figure 1Bb). The needle track shown in Figure 1Bb confirmed the precise Arc-targeted injection. Immunohistochemistry revealed a unilateral increase in NPY peptide expression in the Arc of $NPY^{-/-}$ mice (Figure 1Bb).

In addition to these models, we also utilized our NPYCre knockin line, which allows NPY to be specifically expressed only in NPY neurons in the Arc. In this model, the Cre-recombinase gene is under the control of the endogenous NPY promoter. When injected with an AAV-NPY-FLEX vector, this guarantees that Cre-recombinase is only active in NPY neurons and that inversion of the inactive NPY gene in the AAV-NPY-FLEX vector to the active form only occurs in these NPY-expressing neurons. Successful activation of NPY expression in the Arc through this method is shown in Figure 1Bc, with NPY neurons indicated by the coexpression of mCherry (red) and NPY derived from the viral vector visualized by immunohistochemistry (green).

Consistent with previous results (Lin et al., 2006), vector-mediated NPY expression was seen as early as day 3 after injection and was stable for at least 6 months, at which time the expression was still confined to the Arc (data not shown). In keeping with our histological confirmation of successful reintroduction or overexpression of NPY in the Arc, body weight of our models was markedly increased over the 8 weeks after the injection period, as compared to their corresponding controls (Figure S1A available online). Interestingly, however, body weight gain in the Arc reintroduced models on an otherwise NPY-deficient background was significantly less than that of WT mice

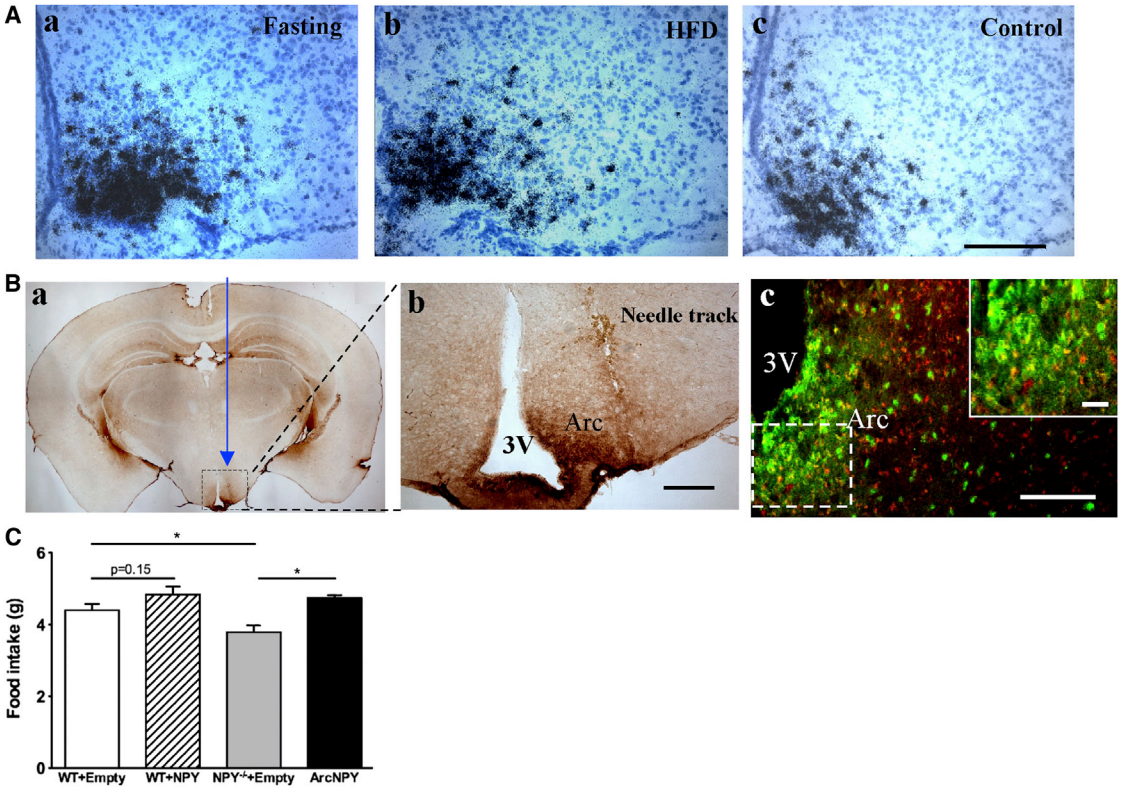

Figure 1. Arc NPY Expression under Various Conditions

(A) ^{35}S-labeled in situ hybridization shows NPY mRNA expression in the Arc of WT mice fasted for 24 hr (a), (b) after 20 weeks of high-fat diet (HFD) (b), and nonfasted chow-fed WT mice (c). The scale bar represents 60 μm.

(B) Shown in (a) is a photomicrograph of coronal brain section showing immunostaining of NPY after unilateral injection of AAV-NPY virus into the Arc of NPY$^{-/-}$ mice (on the right side). Shown in (b) is a higher-magnification of boxed area in (a) showing the needle track just outside the Arc (the scale bar represents 40 μm). Shown in (c) is a representative photomicrograph of coronal brain section showing successful NPY restoration only into NPY neurons of the Arc of NPYCre knockin mice with an AAV-FLEX-NPY vector. The reintroduced NPY is detected with immunohistochemistry with an antibody coupled to a green fluorescence protein seen as yellow due to the overlap of colocalized red fluorescence of the mCherry gene only expressed in NPY-expressing neurons. The scale bar represents 40 μm. Inset is a higher magnification of the boxed area; the scale bar represents 25 μm. 3V, the third cerebral ventricle; Arc, arcuate nucleus.

(C) Daily food intake measured 1 week after AAV virus injection. Data are means ± SEM. n = 8–10 mice per group. *$p < 0.05$ versus genotype-matched AAV-empty or for the comparisons indicated by horizontal bar.

See also Figure S1.

overproducing NPY in the Arc, suggesting that extra-Arc sources of NPY are also critical for increasing body weight. Importantly, there was no significant difference between the *ArcNPY* and the Arc-FLEX-NPY groups with regard to body weight and other parameters described below, suggesting the effects of NPY in the *ArcNPY* model are mediated by NPY neurons. However, since overexpression of NPY in WT, Y1$^{-/-}$, Y2$^{-/-}$, and Y1$^{lox/lox}$ mice, all of which were used in this study, was not possible with the AAV-FLEX-NPY virus, all comparisons below are shown between *WT+NPY* or *ArcNPY* and the respective AAV-empty controls.

Arc Only NPY Signaling Directly Decreases Whole-Body Energy Expenditure

In order to investigate the direct consequences of Arc NPY signaling on energy expenditure while avoiding potential secondary effects that could be caused by the marked increases in body weight that occur over a longer period of time (Figure S1A), we analyzed *WT+NPY* and *ArcNPY* mice within the first 3 weeks after viral delivery. Mice were monitored for body weight, energy expenditure, and food intake. At day 8 after injection, *NPY*$^{-/-}$*+empty* mice consumed significantly less food than did the *WT+empty* mice (Figure 1C). Importantly, however, food intake was increased over *WT+empty* values in the *WT+NPY* and *ArcNPY* mice, with *ArcNPY* mice also consuming significantly more than their corresponding controls, confirming the functionality of the virally delivered NPY (Figure 1C). Despite this increase in 24 hr food intake, body weight (Figure S1B) and whole-body fat mass (Figure S1C) were not significantly different from those of mice in the *WT+empty* or *NPY*$^{-/-}$*+empty* groups.

Strikingly, despite similar body weight and adiposity, oxygen consumption (Figure 2A) and carbon dioxide (CO_2) production (Figure S1D) in *WT+NPY* and *ArcNPY* mice were reduced compared to the corresponding control values (Figure 2A). These changes were associated with a significant reduction in energy expenditure in both genotypes (Figure 2B), indicating a direct inhibitory action caused by Arc NPY signaling. These findings strongly suggest that Arc NPY reduces energy

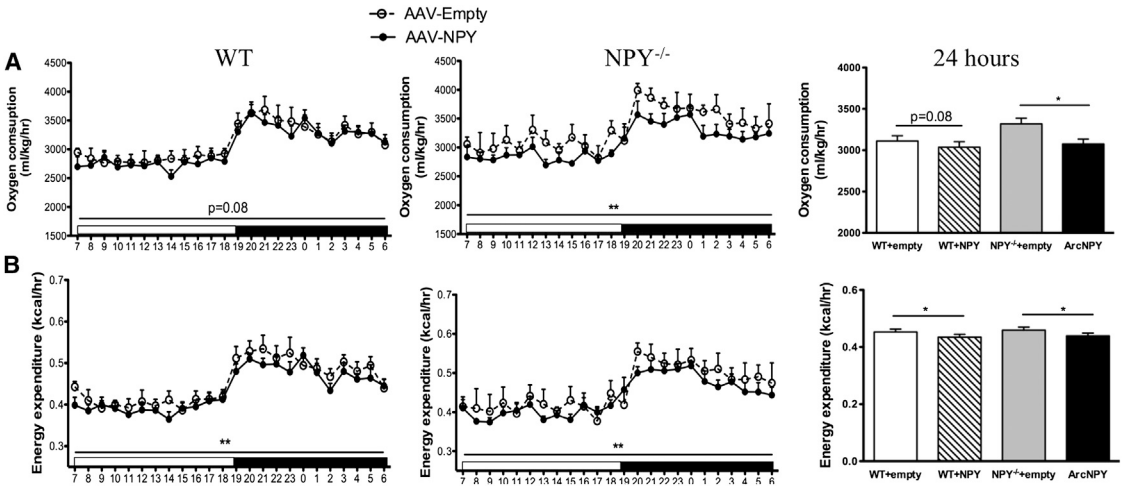

Figure 2. Effects of Arc NPY Signaling on Oxygen Consumption and Energy Expenditure in WT and NPY$^{-/-}$ Mice

Oxygen consumption (A) and energy expenditure (B) measured by indirect calorimetry 1 week after injection with AAV-empty or AAV-NPY vectors into the Arc of 13-week-old WT and NPY$^{-/-}$ mice, respectively. Open and black horizontal bars indicate light and dark phases, respectively. Average oxygen consumption and energy expenditure over total 24 hr period were also calculated and are shown as bar graphs. Data are means ± SEM. n = 5–8 mice per group. *p < 0.05 and **p < 0.01 versus genotype-matched AAV-empty controls or for the comparison indicated by horizontal bar. See also Figure S1.

expenditure before significant changes in fat mass and body weight occur, implying that the direct inhibitory effect observed is not simply a consequence of increased body weight or adiposity.

While Arc NPY signaling had significant short-term effects on oxygen consumption and energy expenditure, there was no major effect of Arc NPY signaling on physical activity in WT or NPY$^{-/-}$ mice (Figure S1E). However, respiratory exchange ratio (RER), an index of oxidative fuel source in *NPY*$^{-/-}$*+empty* mice, was significantly lower than that in *WT+empty* mice, with *ArcNPY* mice showing a trend to reverse this effect on RER (p = 0.1), which is particularly evident during the dark phase (Figure S1F).

Taken together, these observations demonstrate that Arc NPY signaling directly inhibits energy expenditure independently of changes in body weight without major influences on physical activity and show that Arc NPY might have a role in fuel source selection, which could potentially impact on energy expenditure. These differences in energy expenditure also point to the possibility that the Arc-NPY-induced reduction in energy expenditure may be associated with modulation of body temperature. However, rectal temperatures of *WT+NPY* and *ArcNPY* mice in the short-term experiment were not different from those of genotype-matched control mice (data not shown). More-sensitive measures of temperature were thus conducted.

Arc Only NPY Signaling Decreases BAT Temperature

Since levels of NPY are strongly influenced by stress, we utilized a noninvasive high-sensitivity infrared imaging camera to monitor the temperature of interscapular BAT (T_{BAT}), as indicated by the temperature of the overlaying skin in comparison with body temperature represented by lumbar skin temperature of freely moving animals (T_{Back}). These experiments were done 10 days after Arc NPY administration. There was no difference in BAT temperature between *WT+empty* and *NPY*$^{-/-}$*+empty* mice (Figures 3A and 3B). However, *WT+NPY* mice displayed a significant reduction in BAT temperature compared to *WT+empty* control mice (Figures 3A and 3B). Importantly, NPY reintroduction only into the Arc of NPY$^{-/-}$ mice also led to a significant reduction in BAT temperature relative to that of *NPY*$^{-/-}$*+empty* mice (Figures 3A and 3B), demonstrating that NPY signaling in this nucleus alone is able to influence BAT thermogenesis. Lumbar temperature reflecting overall body temperature showed a significant reduction in WT mice upon Arc NPY overproduction but did not reach significance in the NPY reintroduction models (Figure 3B), suggesting that other NPY sources might contribute to this body temperature control.

Arc NPY Signaling Controls POMC and GAD65 but Not AGRP Expression

Having demonstrated the clear link between Arc NPY and energy expenditure and BAT thermogenesis, we next attempted to dissect the neuronal pathways and circuits initiated by Arc-specific NPY signaling. First, we assessed how increased Arc NPY signaling affects the expression levels of other known regulators of energy balance such as POMC and AGRP (Mountjoy, 2010; Ollmann et al., 1997; Tolle and Low, 2008) using in situ hybridization. Unilateral injection of the respective AAV vectors was chosen because it allowed us to use the contralateral side as an internal control. As an additional control, different sets of WT and knockout animals were unilaterally injected with an empty vector (AAV-empty). *NPY*$^{-/-}$*+empty* mice did not show any significant difference from *WT+empty* mice with respect to Arc mRNA expression levels of POMC (Figure 4A). However, compared to the levels in genotype-matched AAV-empty-injected controls, overexpression of NPY targeted to the Arc led to marked reductions in POMC mRNA expression in *WT+NPY* mice (64.5% ± 5.2% versus 100.0% ± 3.2% in *WT+empty*

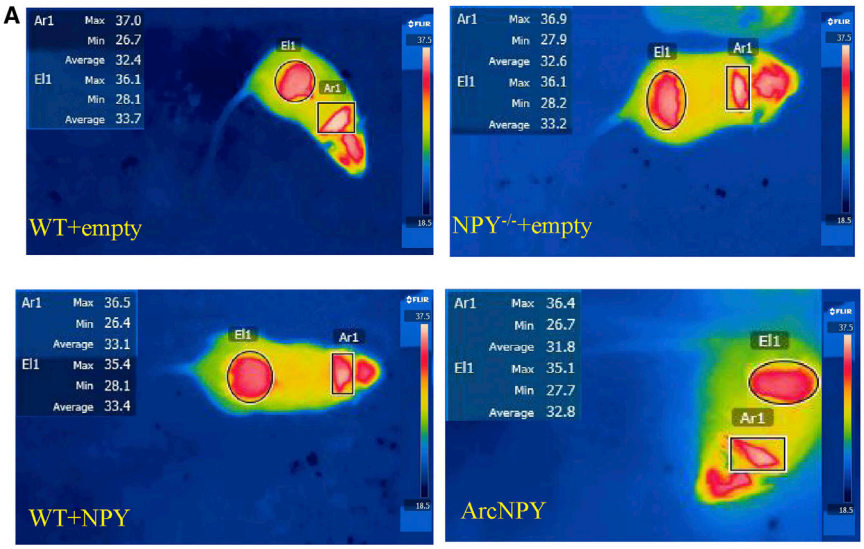

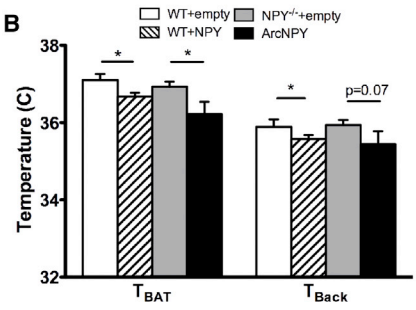

Figure 3. Effect of Arc NPY Signaling on BAT Thermogenesis

(A) Color-coded infrared images visualizing BAT temperatures (rectangular shape, Ar1) and body temperatures (oval shape, El1) of WT and NPY$^{-/-}$ mice injected with either AAV-empty or AAV-NPY into the Arc. Automatically extracted hottest/coldest pixels and average temperature of area of interest are displayed at the top left hand corner of the images. Representative images of 8–10 mice per group.

(B) Average maximum temperature of BAT (T_{BAT}) and average maximum temperature of lumbar back (T_{back}) of WT and NPY$^{-/-}$ mice injected with either AAV-empty or AAV-NPY measured at week 2 after Arc injection. Data are means ± SEM. n = 8–10 mice per group. *p < 0.05 versus genotype-matched AAV-empty.

controls, means ± SEM of five mice per group, p < 0.01) and in *ArcNPY* mice (77.4% ± 8.7% versus 100.4% ± 6.0% in *NPY*$^{-/-}$+*empty* mice, means ± SEM of five mice per group, p < 0.01) (Figure 4A).

It has been suggested that NPY in the hypothalamus may modulate gamma aminobutyric acid (GABA)-ergic activity, and through this pathway indirectly influence POMC expression (Cowley et al., 2001; Horvath et al., 1992; Jegou et al., 1993; Vergoni and Bertolini, 2000). We thus investigated the effect of Arc NPY signaling on mRNA expression of glutamic acid decarboxylase 65 (GAD65), a key enzyme in the synthesis of GABA. Baseline levels of GAD65 mRNA were not significantly different between WT and NPY$^{-/-}$ mice (Figure 4B). However, overproduction or reintroduction of Arc-specific NPY expression resulted in significant elevations in Arc GAD65 mRNA levels in both WT and NPY$^{-/-}$ mice (Figure 4B). This suggests that Arc NPY may enhance GABA production by increasing Arc GAD65 production, which may subsequently contribute to the reduction of POMC mRNA expression. Interestingly, the mRNA expression levels of AGRP, which is coexpressed with endogenous NPY in some Arc neurons and whose expression levels were no different between WT and NPY$^{-/-}$ mice at baseline, did not change upon overproduction or re-introduction of NPY in WT or NPY$^{-/-}$ mice, respectively (Figure 4C). Thus, Arc NPY seems not to be involved in the feedback control of AGRP, suggesting that NPY and AGRP can influence energy homeostasis independently.

Arc NPY Controls Tyrosine Hydroxylase Expression in the PVN

In order to determine other downstream targets of Arc NPY signaling, we next aimed to identify the chemical identity of neurons activated by Arc-specific NPY. Comparing the expression of mRNA of various neurotransmitters in the PVN of lean versus high-fat-diet-fed obese animals, which are known to have elevated Arc NPY levels (Figures 1Aa and 1Ac), we identified tyrosine hydroxylase (TH), the rate-limiting enzyme in the synthesis of catecholamines, as a major candidate on account of its significant downregulation in expression in response to a high-fat diet (Figure 4D). To confirm these PVN TH neurons as targets for Arc NPY signaling, we used our AAV-NPY expression system and overexpressed or reintroduced NPY unilaterally into the Arc of WT and NPY$^{-/-}$ mice. As shown in Figure 4E and quantified in Figure 4F, in both genotypes the elevated expression of NPY in the Arc caused a significant decrease in TH mRNA expression in the PVN only on the injected side (at right in the figure), but not on the contralateral noninjected control side (left) or under conditions of empty virus injection. Importantly, another prominent nucleus of TH expression, the locus coeruleus (LC), also showed significant downregulation of TH mRNA only on the injected side (at right on the figure) and not on the contralateral noninjected control side at left or in empty virus-injected controls (Figures 4E and 4F). Interestingly, the downregulation of TH mRNA in the two nuclei investigated (PVN and LC) was not significantly different between Arc-specific NPY-overexpressing WT and NPY$^{-/-}$ mice (Figure 4F), suggesting that extra-Arc NPY may not play a critical role in the regulation of TH mRNA expression in the PVN or LC. Consistent with the decreased mRNA level of TH in the PVN and LC of Arc-specific NPY overexpressing mice, decreased TH protein expression was also identified in these two nuclei by immunohistochemistry (Figures 5A and 5B). In fact, in the PVN and LC of *ArcNPY* mice, there were 61 ± 9 and 82 ± 8 TH-positive neurons, respectively, in the injected side (at right in Figures 5A and 5B)

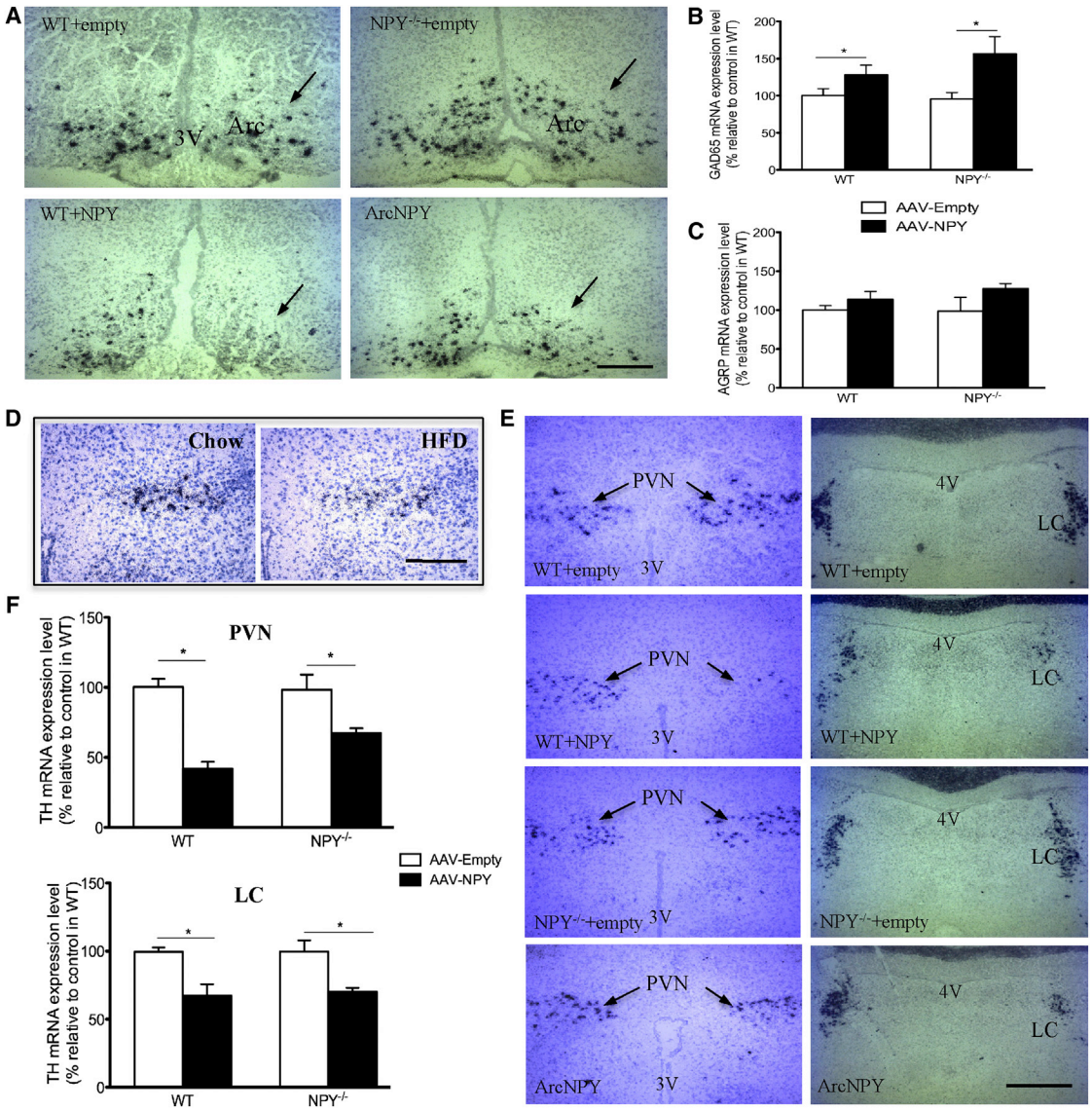

Figure 4. Arc NPY Induced Signaling and Neurotransmitter Regulation

(A) Emulsion-dipped autoradiographs of POMC mRNA expression in the Arc of WT and NPY$^{-/-}$ mice unilaterally injected (on the right side of the figure) with AAV-empty vectors and AAV-NPY vectors. The scale bar represents 40 μm. Images are representative of five to six mice per group. Arc, acuate nucleus; 3V, the third cerebral ventricle.

(B and C) Quantification of GAD65 and AGRP mRNA expression in the Arc, respectively, expressed as a percent of expression level of AAV-empty-injected WT mice. Data are means ± SEM. n = 5–6 mice per group. *p < 0.05 versus genotype-matched AAV-empty controls.

(D) In situ hybridization of TH mRNA in the PVN of WT mice fed with a chow diet or with a high-fat diet for 20 weeks. The scale bar represents 40 μm. Images are representative of n = 5.

(E) Emulsion autoradiographs of TH mRNA expression determined by in situ hybridization in the PVN or locus coeruleus (LC) of WT and NPY$^{-/-}$ mice unilaterally injected (right side) with either AVV-empty or AAV-NPY into the Arc. The scale bar represents 60 μm. 3V, the third cerebral ventricle; 4V, the fourth cerebral ventricle; PVN, paraventricular nuclei.

(F) Quantification of TH mRNA expression in the PVN and LC expressed as a percent of expression level of AAV-empty-injected WT mice. Data are means ± SEM. n = 5–6 mice per group. *p < 0.05 versus genotype-matched AAV-empty controls.

compared to 164 ± 7 and 138 ± 11 TH-positive neurons, respectively, on the contralateral noninjected control side (shown at left). This set of results clearly identifies TH-positive neurons in the PVN and LC as critical downstream targets of Arc NPY signaling and potential mediators of the associated reduction in energy expenditure.

TH Expression in the PVN Is Controlled by Y1 Receptor Signaling

Having established the role of Arc NPY signaling in the control of TH expression in the PVN and LC, we next focused on identifying the Y receptor(s) critical for mediating this action. To achieve this, we initially used germline Y-receptor knockout models

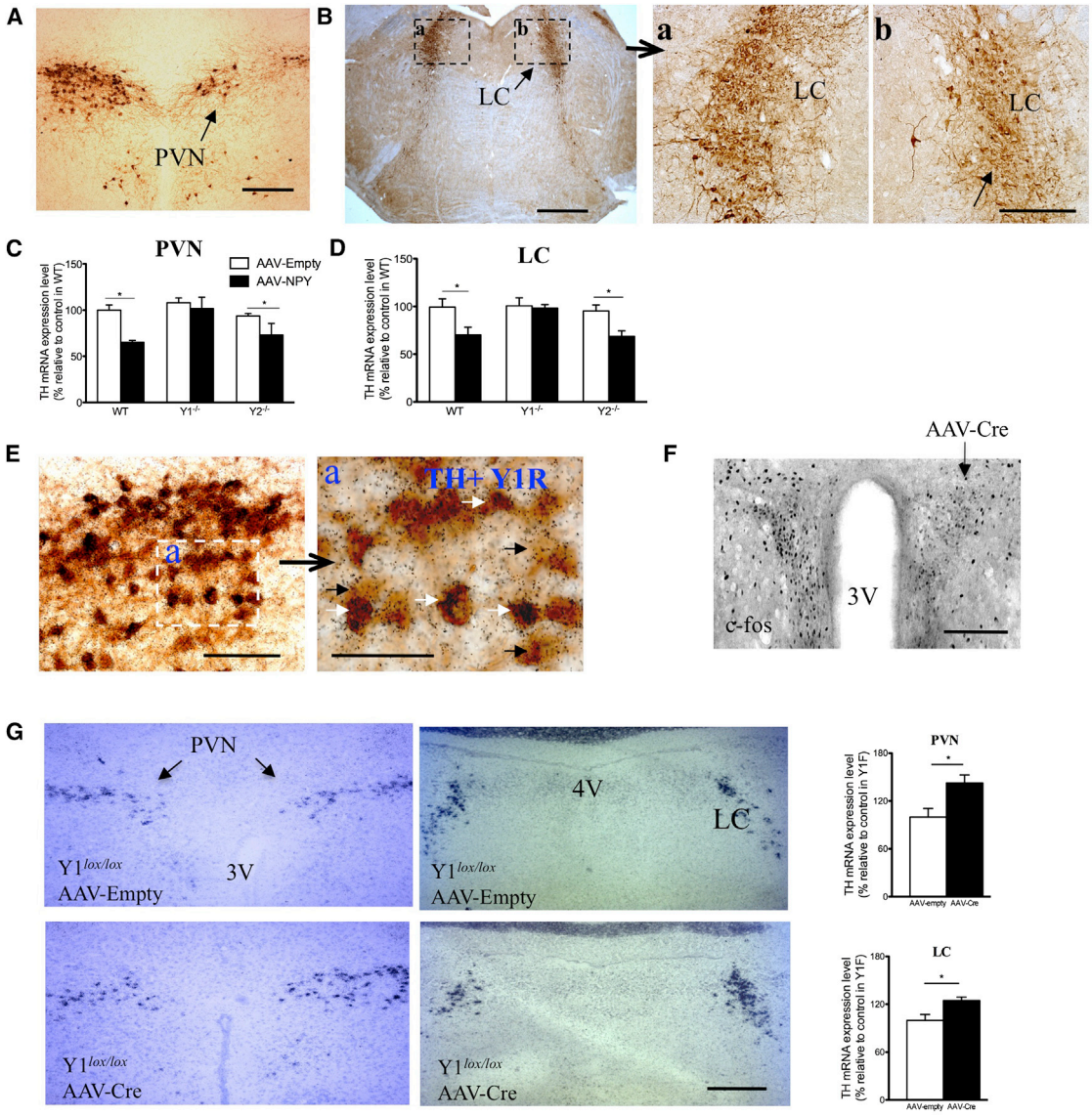

Figure 5. Arc NPY Decreases TH Protein Expression through Y1 Receptor Signaling in TH Neurons of the PVN

(A and B) Immunohistochemistry of TH protein expression in the PVN (A; the scale bar represents 60 μm) and LC (B; scale bar = 100 μm) of NPY$^{-/-}$ mice 4 weeks after unilateral injection (right side) of AVV-NPY into the Arc. (Ba) and (Bb) show the boxed areas in (B) at higher magnification (the scale bar represents 10 μm). Images are representative of five mice per group. PVN, paraventricular hypothalamic nuclei; LC, locus coeruleus.

(C and D) Quantification of TH mRNA expression in the PVN and LC of WT, Y1$^{-/-}$, and Y2$^{-/-}$ mice unilaterally injected into the Arc with AAV-empty or AAV-NPY vectors. Data are means ± SEM. n = 5 mice per group. *p < 0.05 versus genotype-matched AAV-empty-injected control mice.

(E) Double labeling of in situ hybridization for Y1 mRNA and immunohistochemistry for TH expression in the PVN of WT mice. The scale bar represents 25 μm. A higher magnification of the boxed area is shown in (Ea); the scale bar represents 5 μm. Black arrows indicate neurons positive only for TH and white arrows neurons positive for both TH and Y1 receptors.

(F) Bright-field micrograph of reduced c-*fos* expression in unilateral deleted conditional Y1$^{lox/lox}$ mice (right side) followed by i.c.v delivery of $^{[Leu31,Pro34]}$ NPY 4 weeks later. The scale bar represents 40 μm.

(G) Emulsion-dipped autoradiographs of TH mRNA expression in the PVN and the LC of unilaterally injected (right side) Y1$^{lox/lox}$ mice with either AAV-empty vector or AAV-Cre vector, followed by i.c.v. $^{[Leu31,Pro34]}$ NPY 4 weeks later. The scale bar represents 40 μm. Quantification of TH mRNA expression in the PVN and LC is expressed as a percent of expression level of AAV-empty-injected Y1$^{lox/lox}$ control mice. 3V, the third cerebral ventricle; 4V, the fourth cerebral ventricle. Data are means ± SEM. n = 4 mice per group. *p < 0.05 versus AAV-empty-injected control mice.

(Y1$^{-/-}$ and Y2$^{-/-}$ mice) and injected them unilaterally into the Arc with our AAV-NPY virus and using empty vector (AAV-empty) injection as a control. Compared to AAV-empty-injected WT and Y2$^{-/-}$ mice, TH mRNA levels analyzed by in situ hybridization were significantly decreased in the PVN and LC of AAV-NPY-injected WT and Y2$^{-/-}$ mice (Figures 5C and 5D). By contrast, TH mRNA expression in the PVN and LC of AAV-NPY-injected Y1$^{-/-}$ mice did not differ from that of

AAV-empty-injected Y1$^{-/-}$ mice (Figures 5C and 5D). These results suggest that Y1 receptor signaling in TH neurons in the PVN can be directly activated by NPY derived from the Arc, mediating the inhibition of expression of TH mRNA.

To definitively prove that Y1 receptors in the PVN control TH expression, and to establish the sequence of activation of specific TH neuron populations in brain regions, we performed immunohistochemistry for TH combined with in situ hybridization for Y1 receptors. As shown in Figure 5E, a major proportion (68% ± 11%) of TH-immunoreactive neurons in the PVN were also positive for Y1 receptor expression, suggesting that activation of Y1 receptor signaling directly in these cells controls TH expression. To prove this functionally, we next injected conditional Y1 receptor knockout (Y1$^{lox/lox}$) mice unilaterally into the PVN with a Cre-recombinase-expressing AAV vector (AAV-Cre) in order to induce unilateral Y1 receptor deletion in this nucleus. Importantly, 4 weeks after Y1 receptor deletion, i.c.v. injection of the Y1 receptor-preferring agonist $^{[Leu31,Pro34]}$NPY showed a significant reduction in c-*fos* activation only in the deleted site of the PVN compared to the nondeleted contralateral side (Figure 5F, 54 ± 7 c-*fos*-expressing nuclei in the Y1-receptor-deficient side at right in the figure versus 101 ± 12 in the control side at left; data are means ± SEM of four mice per group, p = 0.005). Importantly, mice unilaterally depleted of Y1 receptors in the PVN, when i.c.v. injected 4 weeks later with the Y1 receptor-preferring agonist $^{[Leu31,Pro34]}$NPY, showed higher TH mRNA expression in the Y1 receptor depleted side of the PVN and LC (at right of each panel in Figure 5G) compared to the noninjected contralateral side of each nucleus (at left). By contrast, there was no difference between the injected and noninjected sides of the PVN and LC in brains of mice injected with the AAV-empty control vector (Figure 5G). The elevated PVN and LC TH mRNA expression seen in the Y1-deficient side of the brain also translated into an increase in TH protein levels in the corresponding side of the PVN and LC (Figures 6A and 6B). Importantly, this pattern of increased TH mRNA and protein expression on the side of the unilateral Y1 depletion in the PVN can also be seen in the nucleus of tractus solitarius (NTS) and in the C1/A1 adrenergic or noradrenergic neurons in the ventrolateral medulla (VLM) of the brainstem (Figure 6C), suggesting that NPY signaling on Y1 receptors in the PVN decreases catecholamine synthesis in this nucleus which subsequentially also triggers a reduction in TH production in the LC and other brainstem areas, potentially leading to decreased sympathetic outflow.

Arc NPY Signaling Controls UCP1 Expression in BAT

To further verify our hypothesis that increased Arc NPY-ergic tone can influence SNS activity, we chose to investigate the activity of BAT as it is known to be an intensely sympathetically innervated peripheral target tissue (Lever et al., 1988). First, we carried out bilateral surgical sympathetic denervation (Engel et al., 1992) of BAT to confirm the critical input from these neurons on this tissue and we measured the changes in protein levels of uncoupling protein 1 (UCP1) in BAT as an indication of changes in activity. While baseline protein levels of UCP1 were significantly increased in NPY$^{-/-}$ compared to WT mice, BAT denervation significantly reduced UCP1 levels in both genotypes (Figure 7A), confirming sympathetic activity as a major contributor to UCP1 protein expression. In addition, we also investigated the protein expression levels of peroxisome proliferator-activated receptor-γ coactivator (PGC1α), a key transcriptional regulator of UCP1 whose expression has been reported to be increased in response to activation of the sympathetic nervous system (Puigserver et al., 1998). Interestingly, PGC1α protein levels were not different among sham-operated and denervated groups of WT and NPY$^{-/-}$ mice (Figure 7B), suggesting little or no involvement of PGC1α in the Arc NPY induced sympathetically mediated regulation of BAT UCP1 expression.

Similar to the denervation experiment shown in Figure 7A, lack of NPY, as in *NPY*$^{-/-}$+*empty*-injected mice, led to a strong increase in the UCP1 mRNA (Figure 7C) and protein (Figure 7D) expression in the BAT compared to corresponding values in *WT*+*empty* mice, with quantification shown in Figure 7E. More importantly, Arc injection of NPY in either WT or NPY$^{-/-}$ mice markedly and significantly reduces UCP1 mRNA and protein expression in BAT (Figures 7C–7E). Indeed, there was a nearly 3-fold reduction in BAT UCP1 mRNA expression in *ArcNPY* relative to *NPY*$^{-/-}$+*empty* mice, consistent with a direct effect of Arc NPY signaling on BAT function. Furthermore, we also investigated the expression of PGC1α in BAT in response to Arc NPY signaling. Similar to the denervation experiments, there was no significant difference in PGC1α protein level in the *ArcNPY* group compared to the other three groups (Figure 7D, quantified in Figure 7F), albeit there was a trend to a reduction in PGC1α protein expression in *ArcNPY* mice compared to *NPY*$^{-/-}$+*empty* controls (p = 0.07), suggesting that reduction of UCP1 expression induced by elevated Arc NPY is not necessarily mediated by action of PGC1α in BAT.

To further validate our hypothesis that the alterations of BAT activity were influenced by NPY signaling via Y1 receptors, we also injected germline Y1$^{-/-}$ mice with AAV-empty (*Y1*$^{-/-}$+*empty*) or AAV-NPY (*Y1*$^{-/-}$+*NPY*) into the Arc and investigated the expression of UCP1 and PGC1α in BAT. At baseline, mice lacking the Y1 receptor, as in *Y1*$^{-/-}$+*empty* mice, exhibited upregulated UCP1 protein levels compared to *WT*+*empty* mice (Figure 7E). In contrast to the marked reduction in BAT UCP1 protein expression seen in *WT*+*NPY* and *ArcNPY* mice, *Y1*$^{-/-}$+*NPY* mice showed no such decreases relative to *Y1*$^{-/-}$+*empty* mice (Figure 7E), and there was also no difference in the levels of PGC1α either (Figure 7E). These findings, together with our discovery of the effect of Y1 receptor deletion in the PVN on TH expression (Figures 5A and 5C), confirms that Y1 receptors in the brain, particularly in the PVN, are critical for the inhibitory action of Arc NPY on UCP1 expression in BAT.

DISCUSSION

This study demonstrates that Arc NPY-induced signaling is critical for the control of the hypothalamic and brainstem TH systems that modulate sympathetic outflow, and subsequently energy expenditure including BAT thermogenesis. Results generated by our Arc-only NPY expression models suggest that while Arc NPY has an important role in stimulating feeding, most likely involving alterations in GAD65 and POMC activities in the hypothalamus, which will lead to obesity over time, the control of food intake is not the only critical function of Arc NPY. Indeed, we found that Arc-derived NPY could directly

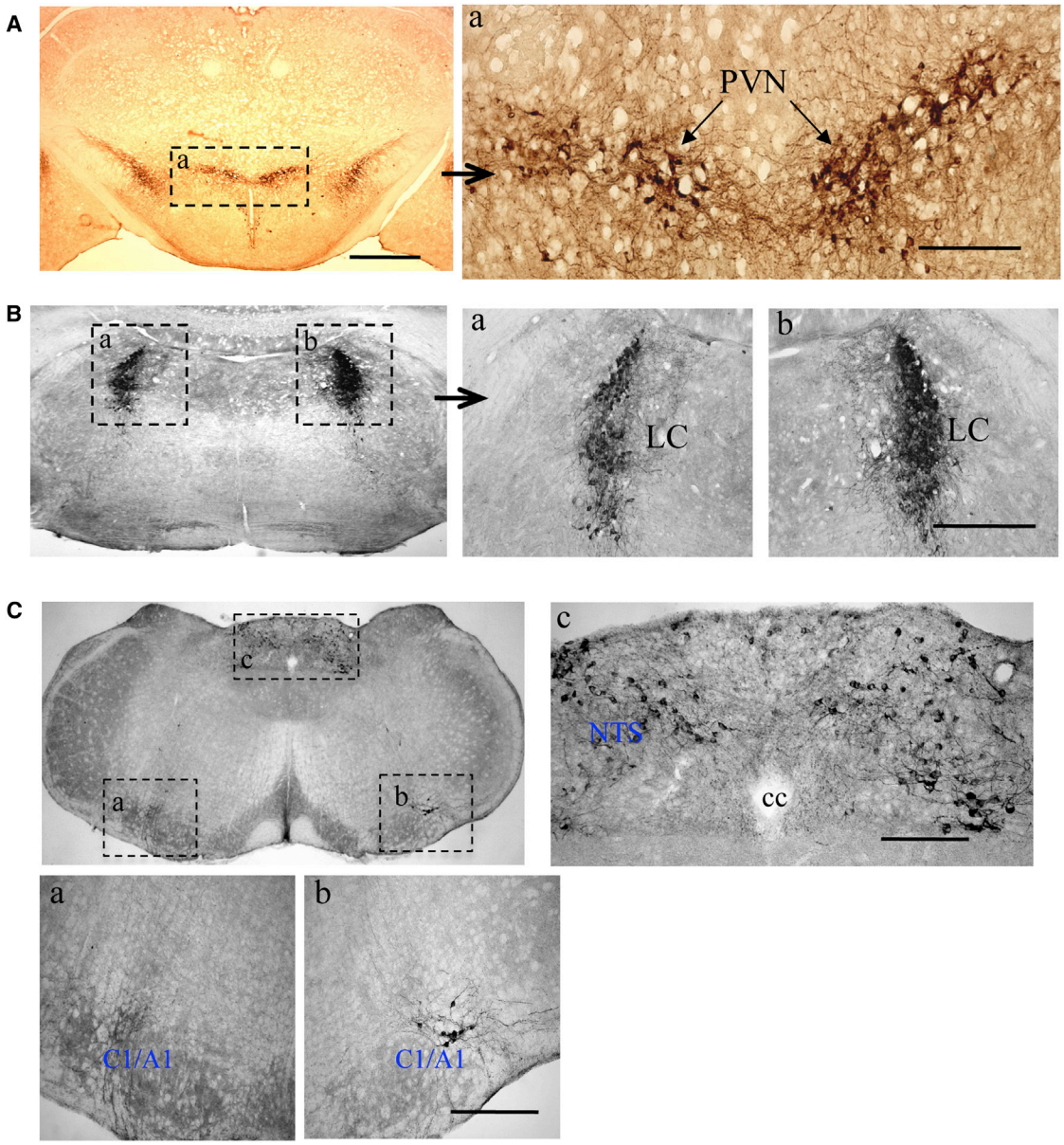

Figure 6. Y1 Receptors Signaling Controls TH Protein Levels in the PVN, LC, NTS, and A1/C1 Neurons

Immunohistochemistry of TH protein expression in the PVN (A), the LC (B), and the NTS (C) and A1/C1 region of $Y1^{lox/lox}$ mice unilaterally injected with AAV-Cre (right side) followed by i.c.v injection of 1.5 μl $^{[Leu31,Pro34]}$ NPY 4 weeks later. The scale bar represents 100 μm. Subpanels show higher magnifications of the boxed areas; scale bars represent 40 μm. Images are representative of five mice. PVN, paraventricular nucleus; LC, locus coeruleus; NTS, nucleus of tractus solitarius; C1/A1, adrenaline neurons/noradrenaline neurons; 3V, the third cerebral ventricle; 4V, the fourth cerebral ventricle; Cc, central canal.

control whole body energy homeostasis, as evidenced by a rapid and robust reduction in energy expenditure in *ArcNPY* mice well before body weight and adiposity were significantly increased. The central mechanism behind this direct control of energy expenditure initiated by Arc NPY is likely due to decreased sympathetic nervous system activity, as shown by decreased TH mRNA and protein expression in the PVN, LC, and brainstem. Importantly, we identified Y1 receptors colocalized on TH neurons in the PVN as the relay point, making it unlikely that Arc NPY directly influences TH levels in the LC and other regions in the brainstem. Consistent with a significant decrease in activity of TH-expressing neurons in the brain, we also demonstrated that this Arc-specific alteration of NPY signaling led to a significant temperature reduction in BAT in association with a downregulation of BAT UCP1 expression, which could be reversed after surgical sympathetic denervation to BAT. Therefore, these data show a causal relationship between Arc NPY signaling and the sympathetic nervous system activity. The potential pathways, neurotransmitters and mechanisms by which Arc NPY signaling may influence food intake, BAT thermogenesis and energy expenditure are summarized in Figure S2.

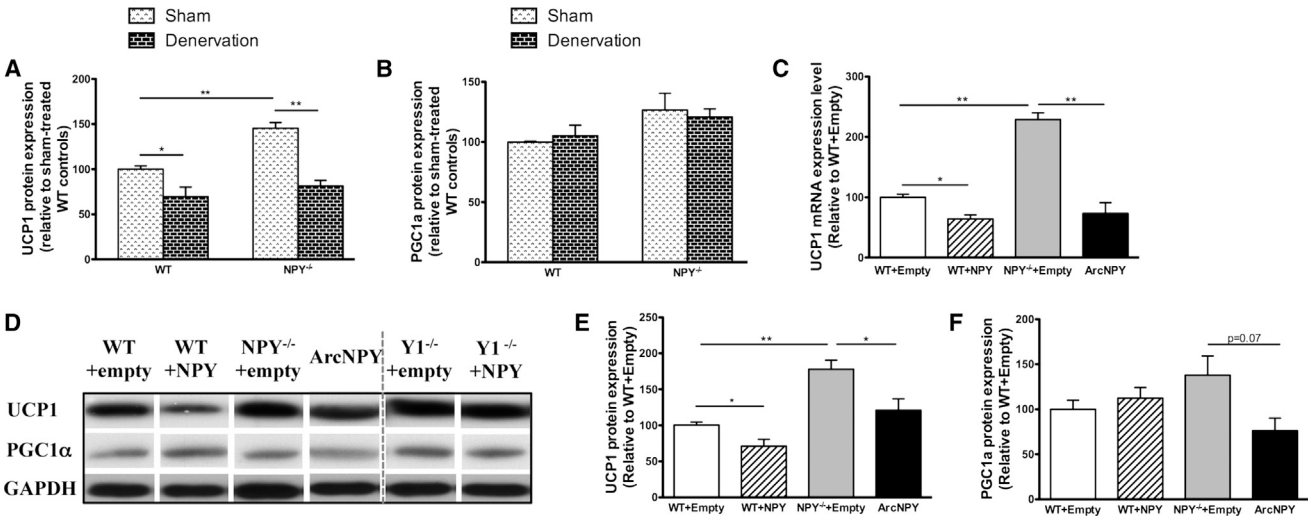

Figure 7. Effects of Arc NPY Signaling on BAT UCP1 and PGC1α Expression

(A and B) Protein levels of UCP1 (A) and PGC1α (B) 3 weeks after bilateral sympathectomy of BAT of WT and NPY$^{-/-}$ mice. The sham-operated genotype-matched mice were used as controls. Data are means ± SEM. n = 5–7 mice per group. *p < 0.05, **p < 0.01 versus genotype-matched controls or for the comparison indicated by horizontal bar.

(C) UCP1 mRNA expression levels in the BAT of WT or NPY$^{-/-}$ mice 3 weeks after being injected into the Arc with either AAV-empty or AAV-NPY. The values were expressed as a percent of expression level of *WT+empty* mice.

(D) UCP1 and PGC1α protein levels in the BAT of WT or NPY$^{-/-}$ mice 3 weeks after being injected into the Arc with either AAV-empty or AAV-NPY determined by western blot. Images are representative of four to five mice per group. GAPDH is used as a loading control.

(E and F) quantification of UCP1 and PGC1α protein expression in the BAT 3 weeks after Arc injection of AAV-empty or AAV-NPY vectors into of WT, NPY$^{-/-}$, and Y1$^{-/-}$ mice, respectively. Data are means ± SEM. n = 5–7 mice per group. *p < 0.05, **p < 0.01 versus genotype-matched controls or for the comparison indicated by horizontal bar.

NPY-ergic tone in the Arc is increased during periods of energy deficiencies, and this is associated with the promotion of food consumption and conservation of energy. However, under the condition of oversupplied nutrition in high-caloric-diet-fed rodents or humans, elevated rather than decreased NPY levels mislead the brain and worsen the symptoms of the metabolic syndrome. In addition, elevation of Arc NPY expression during weight loss after energy restriction may be a strong factor in preventing further weight loss. In this study, experimental elevation of NPY in the Arc mimics these different conditions, allowing us to dissect the downstream neuronal circuits controlled by this altered Arc NPY signaling. Although Arc NPY neurons project to several regions in the brain, the projection to PVN TH-expressing neurons seems to be the most important one for reducing sympathetic activity and thereby modulating energy expenditure. Interestingly, our findings on Arc NPY control of sympathetic output is consistent with a recent report that chemical stimulation of the Arc in rats altered cardiovascular responses by modulating sympathetic nerve activity in the PVN (Kawabe et al., 2012).

Our data show that the phenotypes related to BAT function in *WT+NPY* and *ArcNPY* mice are very similar, suggesting that extra-Arc NPY may not be critical in altering sympathetic outflow relevant to BAT activity. However, potential actions of extra-Arc NPY, either in the brain or in the periphery, cannot be completely ruled out. Indeed, a recent study in rats showed that virus-mediated overexpression of NPY in the DMH leads to body weight gain associated with hyperphagia (Yang et al., 2009). Furthermore, it was also shown that knockdown of NPY in the DMH of rats promotes the development of brown adipocytes in typical WAT depots through sympathetic actions, and this increases BAT activity and therefore enhances energy expenditure and cold-induced thermogenesis (Chao et al., 2011). However, this could be a rat-specific mechanism, since NPY expression in the DMH of mice under normal conditions is rather low. In addition to the DMH, it has been shown that NPY can directly inhibit neurons in the ventromedial nucleus (VMH), a crucial brain region that suppresses food intake (King, 2006). It is also possible that the lack of intact feedback circuits within the brain or from peripheral tissues contributes to the differences in metabolic effects of Arc NPY seen in WT and otherwise NPY-deficient mice. In particular, the observed difference in body weight between WT and NPY$^{-/-}$ mice after chronic overproduction of NPY in the Arc highlights the importance of the entire NPY system for achieving overall control of energy homeostasis.

The identification of TH-expressing neurons in the PVN, a critical brain region for the integration of neuroendocrine and autonomic signals (Swanson and Sawchenko, 1980), as a major target of Arc NPY action is a vital clue for understanding the complex network of neurons regulating energy homeostasis. Our data clearly demonstrate that Y1 receptor signaling in TH-expressing neurons in the PVN suppresses the expression of TH, and through this the activity of indices of sympathetic nervous activity such as BAT temperature and BAT UCP1 expression. Located in the lateral parvocellular subregions of the PVN, TH neurons are known to project to brainstem and spinal cord autonomic regulatory centers and to integrate sympathetic/parasympathetic outflow (Swanson and Sawchenko,

1983). Furthermore, PVN anterograde tracing studies have demonstrated that the LC is a primary target of neuronal projections from the PVN (Reyes et al., 2005; Zheng et al., 1995). As the rate-limiting enzyme in the biosynthesis of the catecholamines dopamine, noradrenaline, and adrenaline, TH forms the primary control mechanism for the production of catecholamines. While PVN TH-positive neurons are most likely dopaminergic, the LC consists of a compact population of TH-positive neurons that are exclusively noradrenergic, readily identifiable by their expression of catecholamine-synthetic enzymes (Geerling et al., 2010). In addition, LC noradrenergic neurons project to a variety of other areas of the brain, including the hypothalamus, amygdala, hippocampus, and striatum, where they are involved in regulating stress responses and stress-related vigilance and arousal, not uncommon conditions associated with elevated Arc NPY levels mimicking negative energy balance. Importantly, it has also been shown that TH-positive neurons in the PVN directly project to brainstem autonomic regions such as the NTS and A1/C1 cell groups (Geerling et al., 2010). From there, the catecholamine-synthesizing neurons in the brainstem send efferent signals to the spinal cord and control many autonomic organs, including BAT, to regulate SNS-mediated thermogenesis and peripheral tissue metabolism.

Taken together, our data have demonstrated that increased NPY expression in the Arc as commonly seen under fasting, stress, or chronic-overfeeding conditions, acting via PVN Y1 receptors, results in a functional inhibition of TH tonus and BAT thermogenesis. Our results also show the inhibitory function of Arc NPY signaling in controlling POMC neurons, probably via altering GAD65 levels, and this likely contributes to increased food intake. Importantly, there was no change in AGRP expression upon Arc NPY administration, suggesting that there is no feedback regulation by NPY on AGRP neurons. This also suggests that AGRP, which is colocalized in some Arc NPY neurons, can act independently of NPY, allowing different components of energy homeostasis to be controlled by the same neurons. This new discovery of the pathways modifying neural sympathetic activity in response to Arc NPY provides greater insights into the hypothalamic regulation of energy homeostasis.

EXPERIMENTAL PROCEDURES

Animals

All animal experiments were conducted in accordance with relevant guidelines and regulations. Male (wild-type, $NPY^{-/-}$, $Y1^{-/-}$, $Y2^{-/-}$, conditional Y1 knockout $Y1^{lox/lox}$, and NPYCre knockin) mice all on a mixed C57Bl6/129SVJ background were used for these experiments. They were housed under conditions of controlled temperature (22°C) with a 12:12 hr light-dark cycle (lights on at 07:00 hr) and fed a standard chow diet with ad libitum access to water, except where noted. Generation of the $NPY^{-/-}$, $Y1^{-/-}$, $Y2^{-/-}$, and conditional $Y1^{lox/lox}$ mice has been described previously (Howell et al., 2003; Karl et al., 2008; Sainsbury et al., 2002; Zhang et al., 2010). NPYCre knockin mice were generated as described in the Supplemental Experimental Procedures.

Viral Vector Injection and Measurement of Body Weight and Fat Mass

Hypothalamic Arc-targeted viral injection was performed as described in the Supplemental Experimental Procedures. The physiological efficacy of viral NPY expression was confirmed by the resultant increase in food intake. Body weight was monitored twice a week at the same time of the day for 3 weeks in the short-term experiment and weekly for the 8 week experiment. Whole-body fat was measured at 13 weeks of age with dedicated dual-energy X-ray absorptiometry (DEXA; Lunar PIXImus2 mouse densitometer, GE Medical Systems, Madison, WI) as described previously (Shi et al., 2011).

Indirect Calorimetry Studies, Food Intake, and Physical Activity

Oxygen consumption rate (VO_2) and carbon dioxide output (VCO_2) were measured 1 week after AAV injection with an indirect calorimeter (Oxymax series; Columbus Instruments, Columbus, OH) as described previously (Shi et al., 2011). In brief, after 24 hr of acclimatization, VO_2, VCO_2, body weight, and daily food intake were measured over a 24 hr period, and the RER and energy expenditure were calculated. Relative physical activity of individually housed mice was also evaluated.

BAT Temperature Measurements with Infrared Imaging

Temperature of interscapular BAT (T_{BAT}) and body temperature was measured by noninvasive high-sensitivity infrared camera (ThermoCAM T640, FLIR) as described in the Supplemental Experimental Procedures. Data were analyzed with the ThermaCAM 7 Pro software calculating the hottest pixel and average temperature of each area of interest.

Intrascapular BAT Bilateral Sympathectomy

Afferent sympathectomy of BAT was carried out in a subset of 11- to 12-week-old male mice immediately after they had been injected with AAV-empty or AAV-NPY virus as described in previously (Engel et al., 1992; Niijima et al., 1984). In brief, with a microscope, intrascapular BAT was exposed by cutting of the overlaying skin and the adjacent muscles. Five sympathetic nerve bundles supplying each lobe of BAT were identified, carefully lifted with forceps, and severed. A similar procedure was performed in sham-operated groups except without sympathetic nerve incision of BAT. The mice were placed on heat pads during surgery and until recovery.

RNA Extraction and Quantitative Real-Time PCR

BAT were dissected and immediately frozen in liquid N_2, and total RNA was isolated with Trizol Reagent and processed for quantitative real-time PCR with the LightCycler system as described in the Supplemental Experimental Procedures.

Western Blotting

BAT samples from all groups were homogenized in RIPA buffer as previously described (Shi et al., 2011), and 20 μg protein was resolved by SDS-PAGE and immunoblotted with antibodies against UCP1 (Alpha Diagnostic International, San Antonio, TX), PGC1α (Calbiochem, Merck, Kilsyth, Australia), and GAPDH. Immunolabelled bands were quantified by densitometry.

In Situ Hybridization

Coronal brain sections (20 μm) were cut on a cryostat and mounted on slides. Matching sections from the same coronal brain level from the four groups of mice (n = 5 mice/group) were assayed together using radiolabelled DNA oligonucleotides complementary to mouse *POMC*, *GAD65*, *AGRP*, *NPY*, and *TH*. Sequence of probes and details of the in situ hybridization methodology can be found in the Supplemental Experimental Procedures.

Immunohistochemistry for Determination of NPY-Induced Changes in the Brain

The mice were anaesthetized and the brains were perfused with saline and then 4% paraformaldehyde (PFA). Brains were postfixed in 4% PFA and then placed in 30% sucrose overnight and cut at 30 μm, and immunohistochemistry was performed as described in the Supplemental Experimental Procedures. After coverslipping, 12 sections from each mouse were visualized and counted for c-*fos* or TH immunoreactivity within the brain nuclei of interest with a Zeiss Axioplan light microscope.

Double Immunostaining and In Situ Hybridization

Five WT male mice were killed and brains were immediately removed and frozen. Coronal brain sections, 20 μm thick, were cut and mounted on slides. Double immunostaining assays were carried out as described in details in the Supplemental Experimental Procedures.

Statistical Analysis

All values are presented as means ± SEM. One- or two-way ANOVA (for body weight, basal food intake, VO_2, VCO_2, energy expenditure, physical activity, and RER) or repeated-measures ANOVA (BAT and lumbar temperature) was used (GraphPad Prism 5, GraphPad Software). Bonferroni post hoc tests were performed to identify differences among means. $p < 0.05$ was considered significant.

SUPPLEMENTAL INFORMATION

Supplemental Information includes Supplemental Experimental Procedures and two figures and can be found with this article online at http://dx.doi.org/10.1016/j.cmet.2013.01.006.

ACKNOWLEDGMENTS

This work was supported by the National Health and Medical Research Council (NHMRC) of Australia with grant number 427661 and fellowships to S.L., A.S., P.B., and H.H.

Received: August 15, 2011
Revised: December 3, 2012
Accepted: January 11, 2013
Published: February 5, 2013

REFERENCES

Baranowska, B., Wolińska-Witort, E., Martyńska, L., Chmielowska, M., Mazurczak-Pluta, T., Boguradzka, A., and Baranowska-Bik, A. (2005). Sibutramine therapy in obese women—effects on plasma neuropeptide Y (NPY), insulin, leptin and beta-endorphin concentrations. Neuroendocrinol. Lett. *26*, 675–679.

Batterham, R.L., Cowley, M.A., Small, C.J., Herzog, H., Cohen, M.A., Dakin, C.L., Wren, A.M., Brynes, A.E., Low, M.J., Ghatei, M.A., et al. (2002). Gut hormone PYY(3-36) physiologically inhibits food intake. Nature *418*, 650–654.

Bray, G.A., and York, D.A. (1998). The MONA LISA hypothesis in the time of leptin. Recent Prog. Horm. Res. *53*, 95–117, discussion 117–118.

Chao, P.T., Yang, L., Aja, S., Moran, T.H., and Bi, S. (2011). Knockdown of NPY expression in the dorsomedial hypothalamus promotes development of brown adipocytes and prevents diet-induced obesity. Cell Metab. *13*, 573–583.

Cowley, M.A., Smart, J.L., Rubinstein, M., Cerdán, M.G., Diano, S., Horvath, T.L., Cone, R.D., and Low, M.J. (2001). Leptin activates anorexigenic POMC neurons through a neural network in the arcuate nucleus. Nature *411*, 480–484.

Egawa, M., Yoshimatsu, H., and Bray, G.A. (1991). Neuropeptide Y suppresses sympathetic activity to interscapular brown adipose tissue in rats. Am. J. Physiol. *260*, R328–R334.

Ellacott, K.L., and Cone, R.D. (2004). The central melanocortin system and the integration of short- and long-term regulators of energy homeostasis. Recent Prog. Horm. Res. *59*, 395–408.

Elmquist, J.K., Ahima, R.S., Elias, C.F., Flier, J.S., and Saper, C.B. (1998). Leptin activates distinct projections from the dorsomedial and ventromedial hypothalamic nuclei. Proc. Natl. Acad. Sci. USA *95*, 741–746.

Engel, B.T., Sato, A., and Sato, Y. (1992). Responses of sympathetic nerves innervating blood vessels in interscapular, brown adipose tissue and skin during cold stimulation in anesthetized C57BL/6J mice. Jpn. J. Physiol. *42*, 549–559.

Geerling, J.C., Shin, J.W., Chimenti, P.C., and Loewy, A.D. (2010). Paraventricular hypothalamic nucleus: axonal projections to the brainstem. J. Comp. Neurol. *518*, 1460–1499.

Hahn, T.M., Breininger, J.F., Baskin, D.G., and Schwartz, M.W. (1998). Coexpression of Agrp and NPY in fasting-activated hypothalamic neurons. Nat. Neurosci. *1*, 271–272.

Horvath, T.L., Naftolin, F., and Leranth, C. (1992). GABAergic and catecholaminergic innervation of mediobasal hypothalamic beta-endorphin cells projecting to the medial preoptic area. Neuroscience *51*, 391–399.

Howell, O.W., Scharfman, H.E., Herzog, H., Sundstrom, L.E., Beck-Sickinger, A., and Gray, W.P. (2003). Neuropeptide Y is neuroproliferative for post-natal hippocampal precursor cells. J. Neurochem. *86*, 646–659.

Jegou, S., Blasquez, C., Delbende, C., Bunel, D.T., and Vaudry, H. (1993). Regulation of alpha-melanocyte-stimulating hormone release from hypothalamic neurons. Ann. N Y Acad. Sci. *680*, 260–278.

Kamegai, J., Tamura, H., Shimizu, T., Ishii, S., Sugihara, H., and Wakabayashi, I. (2000). Central effect of ghrelin, an endogenous growth hormone secretagogue, on hypothalamic peptide gene expression. Endocrinology *141*, 4797–4800.

Karl, T., Duffy, L., and Herzog, H. (2008). Behavioural profile of a new mouse model for NPY deficiency. Eur. J. Neurosci. *28*, 173–180.

Kawabe, T., Kawabe, K., and Sapru, H.N. (2012). Cardiovascular responses to chemical stimulation of the hypothalamic arcuate nucleus in the rat: role of the hypothalamic paraventricular nucleus. PLoS ONE *7*, e45180.

King, B.M. (2006). The rise, fall, and resurrection of the ventromedial hypothalamus in the regulation of feeding behavior and body weight. Physiol. Behav. *87*, 221–244.

Lever, J.D., Mukherjee, S., Norman, D., Symons, D., and Jung, R.T. (1988). Neuropeptide and noradrenaline distributions in rat interscapular brown fat and in its intact and obstructed nerves of supply. J. Auton. Nerv. Syst. *25*, 15–25.

Lin, S., Storlien, L.H., and Huang, X.F. (2000). Leptin receptor, NPY, POMC mRNA expression in the diet-induced obese mouse brain. Brain Res. *875*, 89–95.

Lin, S., Boey, D., and Herzog, H. (2004). NPY and Y receptors: lessons from transgenic and knockout models. Neuropeptides *38*, 189–200.

Lin, E.J., Sainsbury, A., Lee, N.J., Boey, D., Couzens, M., Enriquez, R., Slack, K., Bland, R., During, M.J., and Herzog, H. (2006). Combined deletion of Y1, Y2, and Y4 receptors prevents hypothalamic neuropeptide Y overexpression-induced hyperinsulinemia despite persistence of hyperphagia and obesity. Endocrinology *147*, 5094–5101.

Lundberg, J.M., Rudehill, A., and Sollevi, A. (1989). Pharmacological characterization of neuropeptide Y and noradrenaline mechanisms in sympathetic control of pig spleen. Eur. J. Pharmacol. *163*, 103–113.

Major, G.C., Doucet, E., Trayhurn, P., Astrup, A., and Tremblay, A. (2007). Clinical significance of adaptive thermogenesis. Int J Obes (Lond) *31*, 204–212.

Marks, J.L., Porte, D.J., Jr., Stahl, W.L., and Baskin, D.G. (1990). Localization of insulin receptor mRNA in rat brain by in situ hybridization. Endocrinology *127*, 3234–3236.

Milewicz, A., Mikulski, E., and Bidzińska, B. (2000). Plasma insulin, cholecystokinin, galanin, neuropeptide Y and leptin levels in obese women with and without type 2 diabetes mellitus. Int. J. Obes. Relat. Metab. Disord. *24*(*Suppl 2*), S152–S153.

Mountjoy, K.G. (2010). Functions for pro-opiomelanocortin-derived peptides in obesity and diabetes. Biochem. J. *428*, 305–324.

Nguyen, A.D., Mitchell, N.F., Lin, S., Macia, L., Yulyaningsih, E., Baldock, P.A., Enriquez, R.F., Zhang, L., Shi, Y.C., Zolotukhin, S., et al. (2012). Y1 and Y5 receptors are both required for the regulation of food intake and energy homeostasis in mice. PLoS ONE *7*, e40191.

Niijima, A., Rohner-Jeanrenaud, F., and Jeanrenaud, B. (1984). Role of ventromedial hypothalamus on sympathetic efferents of brown adipose tissue. Am. J. Physiol. *247*, R650–R654.

Ollmann, M.M., Wilson, B.D., Yang, Y.K., Kerns, J.A., Chen, Y., Gantz, I., and Barsh, G.S. (1997). Antagonism of central melanocortin receptors in vitro and in vivo by agouti-related protein. Science *278*, 135–138.

Puigserver, P., Wu, Z., Park, C.W., Graves, R., Wright, M., and Spiegelman, B.M. (1998). A cold-inducible coactivator of nuclear receptors linked to adaptive thermogenesis. Cell *92*, 829–839.

Reyes, B.A., Valentino, R.J., Xu, G., and Van Bockstaele, E.J. (2005). Hypothalamic projections to locus coeruleus neurons in rat brain. Eur. J. Neurosci. *22*, 93–106.

Rosen, E.D., and Spiegelman, B.M. (2006). Adipocytes as regulators of energy balance and glucose homeostasis. Nature *444*, 847–853.

Sainsbury, A., and Zhang, L. (2010). Role of the arcuate nucleus of the hypothalamus in regulation of body weight during energy deficit. Mol. Cell. Endocrinol. *316*, 109–119.

Sainsbury, A., Cusin, I., Rohner-Jeanrenaud, F., and Jeanrenaud, B. (1997a). Adrenalectomy prevents the obesity syndrome produced by chronic central neuropeptide Y infusion in normal rats. Diabetes *46*, 209–214.

Sainsbury, A., Rohner-Jeanrenaud, F., Cusin, I., Zakrzewska, K.E., Halban, P.A., Gaillard, R.C., and Jeanrenaud, B. (1997b). Chronic central neuropeptide Y infusion in normal rats: status of the hypothalamo-pituitary-adrenal axis, and vagal mediation of hyperinsulinaemia. Diabetologia *40*, 1269–1277.

Sainsbury, A., Schwarzer, C., Couzens, M., Fetissov, S., Furtinger, S., Jenkins, A., Cox, H.M., Sperk, G., Hökfelt, T., and Herzog, H. (2002). Important role of hypothalamic Y2 receptors in body weight regulation revealed in conditional knockout mice. Proc. Natl. Acad. Sci. USA *99*, 8938–8943.

Shi, Y.C., Lin, S., Castillo, L., Aljanova, A., Enriquez, R.F., Nguyen, A.D., Baldock, P.A., Zhang, L., Bijker, M.S., Macia, L., et al. (2011). Peripheral-specific y2 receptor knockdown protects mice from high-fat diet-induced obesity. Obesity (Silver Spring) *19*, 2137–2148.

Stephens, M., Ludgate, M., and Rees, D.A. (2011). Brown fat and obesity: the next big thing? Clin. Endocrinol. (Oxf.) *74*, 661–670.

Swanson, L.W., and Sawchenko, P.E. (1980). Paraventricular nucleus: a site for the integration of neuroendocrine and autonomic mechanisms. Neuroendocrinology *31*, 410–417.

Swanson, L.W., and Sawchenko, P.E. (1983). Hypothalamic integration: organization of the paraventricular and supraoptic nuclei. Annu. Rev. Neurosci. *6*, 269–324.

Tolle, V., and Low, M.J. (2008). In vivo evidence for inverse agonism of Agouti-related peptide in the central nervous system of proopiomelanocortin-deficient mice. Diabetes *57*, 86–94.

Vergoni, A.V., and Bertolini, A. (2000). Role of melanocortins in the central control of feeding. Eur J Pharmacol. *405*, 25–32.

Virtanen, K.A., Lidell, M.E., Orava, J., Heglind, M., Westergren, R., Niemi, T., Taittonen, M., Laine, J., Savisto, N.J., Enerbäck, S., and Nuutila, P. (2009). Functional brown adipose tissue in healthy adults. N. Engl. J. Med. *360*, 1518–1525.

Whittle, A.J., López, M., and Vidal-Puig, A. (2011). Using brown adipose tissue to treat obesity - the central issue. Trends Mol. Med. *17*, 405–411.

Yang, L., Scott, K.A., Hyun, J., Tamashiro, K.L., Tray, N., Moran, T.H., and Bi, S. (2009). Role of dorsomedial hypothalamic neuropeptide Y in modulating food intake and energy balance. J. Neurosci. *29*, 179–190.

Zarjevski, N., Cusin, I., Vettor, R., Rohner-Jeanrenaud, F., and Jeanrenaud, B. (1993). Chronic intracerebroventricular neuropeptide-Y administration to normal rats mimics hormonal and metabolic changes of obesity. Endocrinology *133*, 1753–1758.

Zhang, L., Macia, L., Turner, N., Enriquez, R.F., Riepler, S.J., Nguyen, A.D., Lin, S., Lee, N.J., Shi, Y.C., Yulyaningsih, E., et al. (2010). Peripheral neuropeptide Y Y1 receptors regulate lipid oxidation and fat accretion. Int J Obes (Lond) *34*, 357–373.

Zheng, J.Q., Seki, M., Hayakawa, T., Ito, H., and Zyo, K. (1995). Descending projections from the paraventricular hypothalamic nucleus to the spinal cord: anterograde tracing study in the rat. Okajimas Folia Anat. Jpn. *72*, 119–135.